

## TeV ENERGY PHYSICS AT LHC AND IN COSMIC RAYS

A.A. Petrukhin, A.G. Bogdanov  
*National Research Nuclear University MEPhI  
(Moscow Engineering Physics Institute),  
115409, Russia, Moscow, Kashirskoe shosse 31*

### Abstract

Recent results obtained at LHC show deviations from predictions of the Standard Model. Therefore it is appropriate to remind about results obtained in cosmic ray experiments earlier at the same energies (in the center of mass system). In this paper, the comparison of LHC and cosmic ray data is fulfilled and various possibility of their explanation is considered.

### 1 Introduction

Now TeV energy region is being intensively investigated in LHC experiments and various deviations from predictions of the standard model are observed. Some of them are confirmed in further experiments, others are not confirmed. But it is interesting to note that, as a rule, the results obtained in nucleus-nucleus interactions (f.e. so-called imbalanced events <sup>1)</sup>, sharp increasing of

secondary particle multiplicity with energy <sup>2)</sup>) are confirmed. Results obtained in proton-proton interactions (2 TeV resonance <sup>3)</sup>, excess of missing energy and lepton transverse momentum <sup>4)</sup>) are not always confirmed. In this connection it is necessary to remind that TeV energy region is investigated in cosmic rays more than 60 years, and many unusual results were obtained (f.e. alignment, penetrating cascades, Centauros <sup>5)</sup>, various deviations in EAS development <sup>6)</sup>, excess of muon bundles, increasing with energy <sup>7, 8)</sup>). The last effect was observed at accelerator detectors, too, firstly in LEP detectors <sup>9, 10)</sup>, then at LHC detectors <sup>11)</sup>. For explanation of different unusual events various theoretical models were proposed, but none of them can explain all observed events and phenomena. In papers <sup>12, 13, 14)</sup> the model of production of quark-gluon matter blobs with large orbital momentum was proposed, which allows explain all observed experimental data.

## 2 The backgrounds and requirements to new model

The necessity of development of a new model for description of all unusual experimental data is caused by a large amount and contradictoriness of various requirements for their explanation.

The first of them is the cross section. In accelerator experiments, rather rare events (with cross section of nb and even pb) can be measured due to a large intensity of beams. In cosmic ray experiments, the values of the cross section of the order of mb (sometimes  $\mu$ b) can be detected only due to a low intensity of CR flux. Since all observed unusual phenomena have a threshold behaviour (they are detected at TeV energies in the center of mass system, which correspond to PeV energy region in cosmic rays) the simplest way of their explanation is a production of some heavy particles (or states of matter). But in this case geometrical cross section

$$\sigma = \pi \lambda^2 = \pi/m^2, \quad (1)$$

will be very small ( $\sim 10^{-34}$  cm<sup>2</sup> at  $m \sim 1$  TeV). Therefore a transition from point-like quark-quark interactions to multi-quark and gluon interactions is required. In this case, some blob of quark-gluon matter is produced and geometrical cross section will be

$$\sigma = \pi R^2, \quad (2)$$

where  $R$  is an effective size of QGM blob, which cannot be less than one nucleon size, and cross section will be of the order of mb.

The second important point is the energy in the center of mass. Usually even for nucleus-nucleus interactions the energy in the center of mass system is calculated for target of nucleon mass. But for collective interaction of many quarks and gluons the target mass can be more than nucleon mass. Therefore instead of

$$\sqrt{s} = \sqrt{2m_N E} \quad \text{we must use} \quad \sqrt{s} = \sqrt{2m_c E}, \quad (3)$$

where  $m_c$  – some compound mass, which in the first approximation can be determined as

$$m_c = nm_N. \quad (4)$$

The third point is connected with an orbital momentum. Its value and significance strongly increase for collective interactions. As was shown in 15), the value of the orbital momentum is proportional to  $\sqrt{s}$  and calculations 16) showed that its value can reach  $\sim 10^4$ . At such large orbital momentum  $L$ , a big centrifugal barrier must appear:

$$V = L^2/2mR^2. \quad (5)$$

Its value will be large for light quarks ( $u$  and  $d$ ), but small for heavy quarks (f.e. for top-quarks). And though top-quarks are absent in interacting nuclei, but suppression of decays of QGM blob into light quarks gives a time for top-quark pair production in boiling quark-gluon matter and their fly out from the blob. This process decreases the energy  $\sqrt{s}$ , and correspondingly orbital momentum and centrifugal barrier are sharply decreased and the rest part of the blob decays into light quarks. The decay of top-quarks:

$$t(\bar{t} \rightarrow b(\bar{b}) + W^+(W^-)). \quad (6)$$

In their turn,  $b$ -quarks give jets or can decay into  $c$ -quarks.  $W$ -bosons decay into leptons ( $\sim 30\%$ ) and into hadrons (mainly pions)  $\sim 70\%$ . These changes of interaction model allow explain all unusual experimental results obtained both in accelerator and cosmic ray experiments.

### 3 Explanation of unusual results of accelerator experiments

In nucleus-nucleus interactions two undoubted results were obtained. The first, so-called unbalanced events in which dijet symmetry is violated <sup>1)</sup>. In the frame of the considered model these events can be explained very easily. The production and consecutive decay of  $t$ -quark gives  $b$ -quark and  $W$ -boson. Interaction of  $b$ -quark gives jet and the decay  $W$ -boson into pions ( $\sim 10$ ) forms an unbalanced event. Really at the decay of  $t$ -quark kinetic energies are distributed as

$$T_b \approx 65 \text{ GeV} \text{ and } T_W \approx 25 \text{ GeV}.$$

If to take into account fly-out energy of  $t$ -quark,  $T_b$  can be more than 100 GeV and ATLAS experiment's picture will be obtained.

The second, the sharp increasing of secondary particle multiplicity in heavy nuclei interactions <sup>2)</sup>. It is important to underline that this result is obtained for energy in center of mass system, which is calculated for nucleon mass  $\sqrt{s_{NN}}$ . But in frame of the considered model this mass must be larger and LHC results allow evaluate it. In fig.1 possible positions of experimental point are shown.

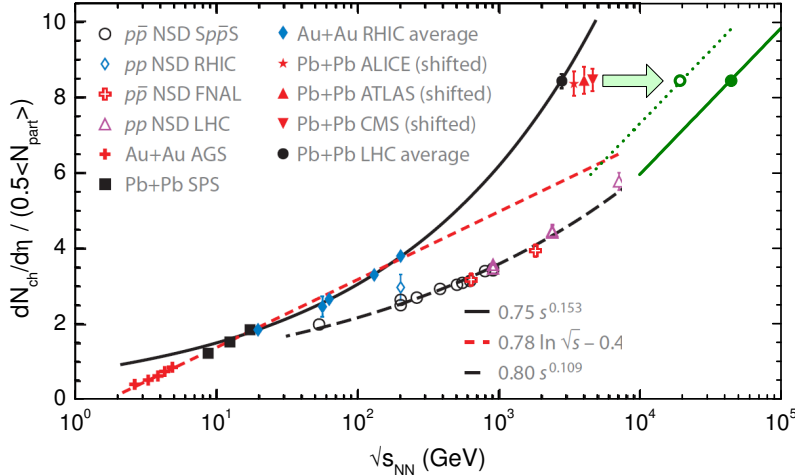


Figure 1: Charged particle multiplicity according to accelerator experiments <sup>2)</sup>.

There are two limiting positions. The upper limit can be evaluated from condition, that  $\sqrt{s_{AA}}$  for nucleus-nucleus interaction cannot be more than  $\sqrt{s_{NN}}$  for  $pp$ -interaction. In this case a number of nucleons in QGM blob

$$\sqrt{n_N} = \sqrt{s_{AA}}/\sqrt{s_{NN}} < 50 \text{ TeV}/3.5 \text{ TeV} \approx 14.$$

This case corresponds to the central collision of nuclei, and target mass is equal to mass of interacting nucleus ( $\sim 200$ ). The lower limit can be evaluated if to assume that the energy dependence of AA-interaction on energy is the same as for  $pp$ -interaction. In this case  $\sqrt{s_{AA}}$  will be about 20 TeV and correspondingly  $\sqrt{n_N}$  will be about 6, and the total number of nucleons in a blob  $\sim 36$ . In this case a target mass is equal to about 1/6 of total target nucleus mass.

It is interesting to compare obtained values with the simplest geometrical models. At low energies nuclei can be considered as spheres and their average region of intersection is shown in fig.2, left.

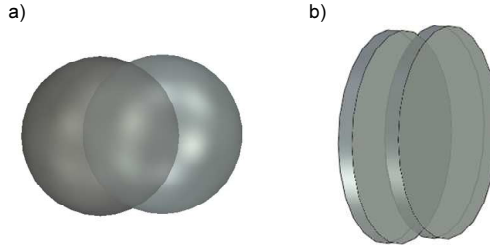


Figure 2: *Region of intersection of two spheres (left) and two disks (right).*

The volume of spherical segment is

$$V = \pi h^2(3R - h)/3. \quad (7)$$

On average,  $h = R/2$  and volume

$$V = \pi \frac{R^2}{4} (3R - \frac{R}{2}) /3 = \frac{4}{3}\pi R^3 (\frac{5}{32}) \approx 0.156 V_{\text{sphere}}.$$

Two volumes will be about  $0.31 \approx 1/3$ . At very high-energies, nuclei can be considered as flat disks and correspondingly the region of intersection will be equal to two flat segments (fig.2, right).

Area of each will be equal to

$$S = h(6a + 8b)/15. \quad (8)$$

For picture in fig.2, right:  $b = R$ ,  $h = R/2$ ,  $a = 2R\sqrt{3}/2 = R\sqrt{3}$ ,

$$S = \frac{R}{2} (6R\sqrt{3} + 8R) / 15 = R^2 (3\sqrt{3} + 4) / 15 \approx \pi R^2 \frac{9.2}{\pi 15} \approx 0.2 S_{\text{disk}}.$$

For two segments, the area will be equal to  $\approx 0.4$  of full nucleus target area. Both values 0.3–0.4 lie in experimental interval 0.17–1.

Very interesting results were obtained using LHC detectors for investigations of cosmic ray muons. Due to a high spatial resolution, these detectors can register muon bundles with big multiplicity. In fig.3 the results of such investigation in ALICE are presented 11).

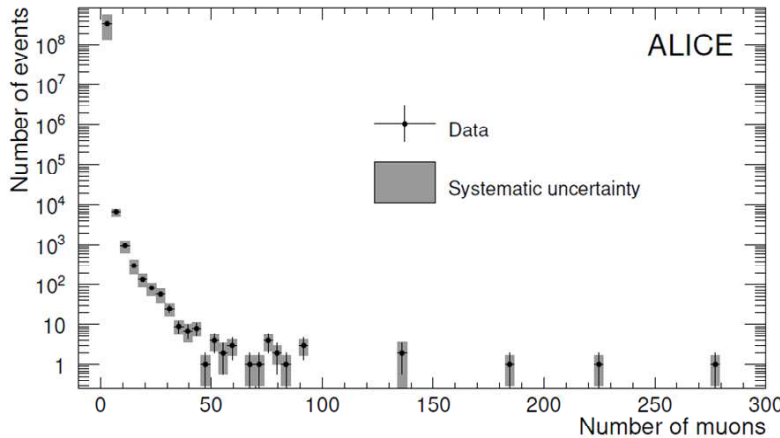


Figure 3: *Atmospheric muon multiplicity distribution in ALICE detector* 11).

A remarkable excess of bundles with high multiplicity (more than 100) was detected. This excess cannot be explained in the frame of traditional process of muon generation in decays of various mesons ( $\pi$ ,  $K$ ,  $D$  etc.). The similar results were obtained earlier at LEP detectors (ALEPH 9), DELPHI 10). Unfortunately, in experiments at accelerator detectors there is no possibility to evaluate the energies of primary particles which are responsible for the appearance of muon bundles with high multiplicity. Such possibility has the experimental complex NEVOD-DECOR 7) (see the next part of the paper).

#### 4 Explanation of CR unusual events

Firstly, it is necessary to underline that cosmic rays consist mainly of nuclei ( $\sim 60\%$ ), if consider their energies per particle (see tab.1). Usual opinion

that cosmic rays consist mainly of protons ( $\sim 90\%$ ) is based on calculations of secondary particle flux in the atmosphere in which a large contribution give leading particles, for that energy per nucleon is important. For EAS measurements, full primary particle energy must be taken into account. Results of EAS investigations show that above the “knee” the part of nuclei is increased. So in cosmic rays most part of interactions are nucleus-nucleus interactions and less part of proton-nucleus interactions.

Table 1: *Composition of cosmic rays at low energies.*

Particles	Z	A	Energy per nucleon	Energy per nucleus
Protons	1	1	92%	40%
$\alpha$ -particles	2	4	7%	21%
Light nuclei	3-5	10	0.15%	3%
Medium nuclei	6-10	15	0.7%	18%
Heavy nuclei	$\geq 11$	32	0.15%	18%

The explanation of various unusual events observed in cosmic rays was given elsewhere <sup>12)</sup>. In this paper the problem of the excess of muon bundles (so-called “muon puzzle”) will be considered only. A serious advancement in investigations of the dependence of muon bundle intensity on primary particle energy was done in experiment NEVOD-DECOR <sup>7)</sup>. In this experiment primary particle energy was evaluated by measurements of zenith angle dependence. In fig.4 the results of inclined muon bundle detection are presented.

From this figure it is seen that at increasing of zenith angle the number of muon bundles is increased in comparison with theoretical calculations at respective zenith angle. Though there is no direct dependence between zenith angle and primary particle energy for each individual event, in general such dependence exists. In fig.5 the results of simulations of the contribution of different primary energies into production of events with fixed local muon density at various zenith angles are presented <sup>7)</sup>.

As one can see from fig.4, the increasing of local muon density starts at energies more  $10^{16}$  eV, which correspond several TeV energies in center of mass system. In principle, this increasing up to energy  $10^{17}$  eV can be explained if CR mass composition becomes heavier. But above  $10^{17}$  eV such explanation is impossible. The further increase of excess of muon bundle number was measured in Pierre Auger Observatory (fig.6 <sup>8)</sup>).

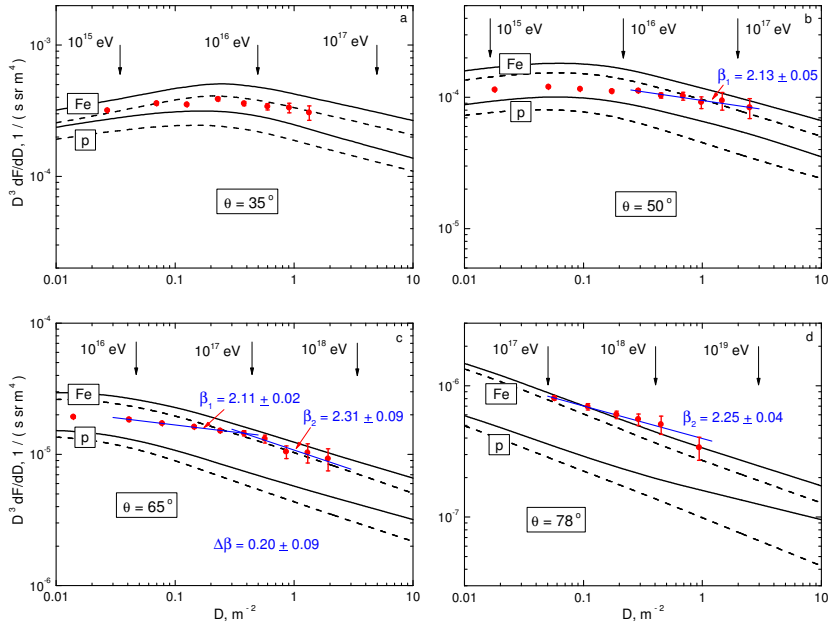


Figure 4: *Experimental (points) and calculated (curves) local muon density spectra for different zenith angles; arrows indicate effective primary energies.*

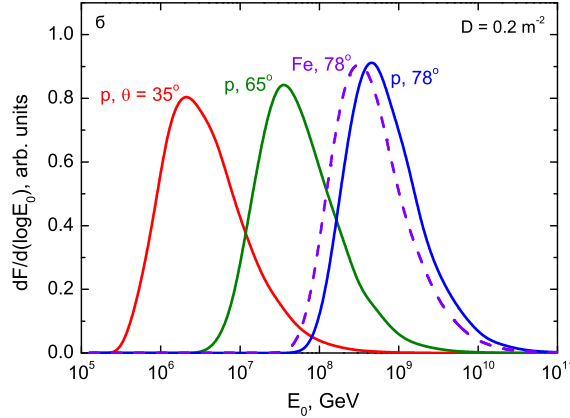


Figure 5: *Contribution of various primary energies into muon bundles flux for fixed local muon density in dependence on zenith angle.*

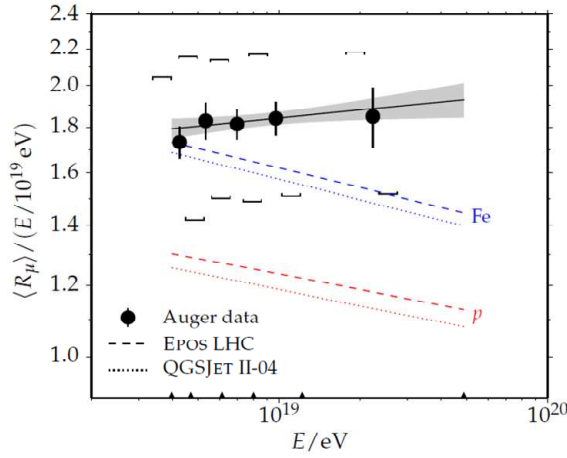


Figure 6: *Results of muon component investigations in Auger experiment* <sup>8)</sup>.

In the model of QGM blobs, the solution of “muon puzzle” is the following. For production of QGM blob not only high temperature (energy) but high quark-gluon density is required. Therefore firstly such blobs will be generated in interactions of heavy particles (iron nuclei) with nuclei of atmospheric atoms. Then, with increasing of primary particle energy, in interactions of more light nuclei. The last will be protons. Of course nucleus interactions have big fluctuations and clear separation of contribution of various nuclei is impossible. But in general the dependence on nucleus mass exists.

Increasing number of QGM blobs with energy and corresponding number of  $W$ -bosons, which mainly decay into pions (on average,  $\sim 20$ ) with not large energy increases the multiplicity of muons bundles.

## 5 Conclusion

Investigations of TeV energy region gave many interesting experimental results. Proposed model of production of QGM blobs with large orbital momentum allows explain all new phenomena observed in this energy region.

## Acknowledgements

Authors thank R.P. Kokoulin for fruitful discussions and the help in preparation of this paper. This work was supported by Ministry of Education and Science of the Russian Federation (government task).

## References

1. G. Aad *et al* (ATLAS Collab.), Phys. Rev. Lett. **105**, 252303 (2010).
2. K. Aamodt *et al* (ALICE Collab.), Phys. Rev. Lett. **105**, 252301 (2010).
3. G. Aad *et al* (ATLAS Collab.), J. High Energy Phys. **12**, 55 (2015).
4. G. Aad *et al* (ATLAS Collab.), J. High Energy Phys. **10**, 150 (2015).
5. S.A. Slavatinsky, Nucl. Phys. B (Proc. Suppl.) **122**, 3 (2003).
6. J. Blumer, R. Engel, J.R. Horandel, Progr. in Part. and Nucl. Phys. **63**, 293 (2009).
7. A.G. Bogdanov *et al*, Phys. Atom. Nucl. **73**, 1852 (2010).
8. A. Aab *et al* (Pierre Auger Collab.), Phys. Rev. D **91**, 032003 (2015).
9. C. Grupen *et al*, Nucl. Phys. B (Proc. Suppl.) **175–176**, 286 (2008).
10. J. Abdallah *et al*, Astropart. Phys. **28**, 273 (2007).
11. J. Adam *et al* (ALICE Collab.), Journal of Cosmology and Astroparticle Physics **1**, 32 (2016).
12. A.A. Petrukhin, Unusual events in PeV energy cosmic rays and their possible interpretation, in: Proc. of the Vulcano Workshop "Frontier Objects in Astrophysics and Particle Physics" (eds. F. Giovannelli, G. Mannocchi, Vulcano Island, Sicily, Italy, May 2004), **90**, 489 (SIF, Bologna, 2005).
13. A.A. Petrukhin, Nucl. Phys. B (Proc. Suppl.) **175–176**, 125 (2008).
14. A.A. Petrukhin, Nucl. Instr. and Meth. in Phys. Res. A **742**, 228 (2014).
15. Z.-T. Liang, X.-N. Wang, Phys. Rev. Lett. **94**, 102301 (2005).
16. J.-H. Gao *et al*, Phys. Rev. G. **77**, 044902 (2008).